European Heart Journal (2004) **25**, 1419–1427

Clinical research

Persistent diastolic dysfunction despite complete systolic functional recovery after reperfused acute myocardial infarction demonstrated by tagged magnetic resonance imaging

Clerio F. Azevedo[a], Luciano C. Amado[a], Dara L. Kraitchman[b], Bernhard L. Gerber[a], Nael F. Osman[b], Carlos E. Rochitte[a], Thor Edvardsen[a], Joao A.C. Lima[a,*]

[a] *Department of Medicine, Division of Cardiology, Johns Hopkins Hospital, 600 N. Wolfe Street/Blalock 524, Baltimore, MD 21287-0409, USA*
[b] *Department of Radiology, Johns Hopkins Hospital, Baltimore, MD, USA*

Received 31 January 2004; revised 10 May 2004; accepted 3 June 2004

KEYWORDS
Myocardial infarction;
Diastole;
Magnetic resonance imaging;
Myocardial stunning

Aims This study was designed to characterise both the systolic and diastolic mechanical properties of regions with different degrees of myocardial ischaemic injury after reperfused acute myocardial infarction (AMI).
Methods and Results Fourteen dogs underwent 90-min coronary artery occlusion followed by reperfusion. Image acquisition was performed 24 h after reperfusion using three techniques: tagged, first-pass perfusion and delayed-enhancement magnetic resonance imaging (MRI). Systolic circumferential strain and both systolic and diastolic strain rates were calculated in 30 segments/animal. Transmural AMI segments displayed reduced systolic contractility when compared to subendocardial AMI segments (systolic strain = $-2.5 \pm 0.5\%$ versus $-6.0 \pm 0.9\%$, $P < 0.01$ and systolic strain rate = -0.11 ± 0.12 versus -0.82 ± 0.16 s^{-1}, $P < 0.01$), and both exhibited significant systolic and diastolic dysfunction compared to remote. Moreover, AMI segments presenting with microvascular obstruction ("no-reflow") displayed further compromise of systolic and diastolic regional function ($P < 0.05$ for both). Importantly, risk region segments only exhibited diastolic impairment (diastolic strain rate = 1.62 ± 0.14 versus 2.99 ± 0.13 s^{-1}, $P < 0.001$), but not systolic dysfunction compared to remote 24 h after reperfusion.
Conclusion Reversibly injured regions can demonstrate persistent diastolic dysfunction despite complete systolic functional recovery after reperfused AMI. Moreover, the presence of no-reflow entails profound systolic and diastolic dysfunction. Finally, tagged magnetic resonance imaging (MRI) strain rate analysis provides detailed mechanical characterisation of regions with different degrees of myocardial ischaemic injury.

* Corresponding author. Tel.: +1-410-614-1284; fax: +1-410-614-8222.
E-mail address: jlima@jhmi.edu (J.A.C. Lima).

0195-668X/$ - see front matter
doi:10.1016/j.ehj.2004.06.024

Introduction

The traditional assessment of global left ventricular (LV) systolic function after acute myocardial infarction (AMI) has important clinical and prognostic significance. However, myocardial injury after AMI is known to be a regional and heterogeneous process.[1] Accordingly, regional functional evaluation has been shown to provide additional important diagnostic and prognostic information over that provided by global assessment alone.

Moreover, ischaemic injury after AMI affects not only systolic but also diastolic function.[2] Indeed, it has been demonstrated that the phenomenon of myocardial stunning[3,4] has both a systolic and a diastolic component.[5] In addition, previous studies have shown that patients presenting with global diastolic dysfunction after AMI have a worse prognosis than those without diastolic impairment and that the prognostic information provided by the diastolic assessment is independent from that derived from the systolic evaluation alone.[6–8] However, initial attempts to quantify regional diastolic function using invasive angiographic studies have been hampered by significant technical complexity and very limited clinical applicability.[6,9] Previous studies using radionuclide[10] and echocardiographic[11–13] techniques have addressed the non-invasive assessment of regional diastolic function but, to our knowledge, none have investigated regional diastolic abnormalities after AMI using tagged MRI strain rate analysis.

Myocardial tagged MRI is currently the non-invasive gold standard method for regional systolic functional evaluation.[14,15] Diastolic assessment by tagged MRI, however, has been limited to the analysis of LV untwisting in early diastole.[16] Using a concept similar to that already used in echocardiography, our group applied the calculation of strain rates for the evaluation of both systolic and diastolic regional function using tagged MRI. Strain rate analysis measures the rate of myocardial contraction and relaxation,[17] as opposed to the magnitude of myocardial systolic and diastolic deformation (myocardial strains).

In this experimental study, we used tagged MRI strain rate analysis to evaluate regional systolic and, particularly, regional diastolic function in areas with different degrees of myocardial injury after reperfused AMI. We examined the hypothesis that this analysis would allow us to better characterise and distinguish these ischaemically injured regions.

Methods

Experimental model

Fourteen adult mongrel dogs (25–30 kg) were anaesthetised, intubated and mechanically ventilated. AMI was created in all animals by a 90-min closed-chest occlusion of either the proximal left anterior descending or the left circumflex coronary artery using an angioplasty balloon. After 90 min the balloon was deflated to allow full reperfusion of the infarcted territory and all animals were followed for 24 h thereafter. The study protocol was approved by the Johns Hopkins Institutional Animal Care and Use Committee and all animals were handled according to the "Guide for the Care and Use of Laboratory Animals".

MRI protocol

All images were acquired 24 h after reperfusion using a 1.5T Signa CV/i scanner (GE Medical Systems, Waukesha, WI). Tagged images were acquired with an ECG-gated, segmented *k*-space, fast gradient-echo pulse sequence with spatial modulation of magnetisation to generate a grid tag pattern. Eight contiguous short-axis slices were prescribed to cover the entire LV from base to apex. In order to be able to depict regional diastolic deformation accurately, the protocol was optimised to provide a tagging sequence with high temporal resolution. Imaging parameters were as follows: tag separation 6.5 mm, 28 cm field of view, 8 mm slice thickness, matrix size 256×160, repetition time 5.5 ms, echo time 1.4 ms, flip angle $a=12^{\circ}$, temporal resolution 22 ms. The temporal profile of each animal during the acquisition of the tagged MRI dataset is presented in Table 1.

After completion of the tagged imaging sequence, an intravenous bolus injection of 0.1 mmol/kg gadolinium-DTPA (Magnevist, Berlex) was administered for first-pass perfusion imaging.[18] The acquisition started simultaneously with contrast injection, and images were acquired continuously for ~80 s with two consecutive breath-holds (~40 s duration each). After first-pass perfusion image acquisition, a second bolus of 0.1 mmol/kg gadolinium-DTPA was given. Delayed-enhanced images were acquired 15 min after second contrast injection using a previously described inversion recovery fast gradient-echo pulse sequence.[19] Both first-pass and delayed-enhanced images were acquired in the identical short-axis locations as the tagged images.

Radioactive microspheres blood flow analysis

Myocardial blood flow was measured at baseline, during coronary artery occlusion and after reperfusion to determine the areas at risk and the regions of microvascular obstruction. For each measurement $\sim 2\times10^{6}$ radioactive microspheres (15–16 lm diameter) labeled with ^{113}Sn, ^{46}Sc, ^{57}Co, or ^{114}Ru (New England Nuclear) were injected into the left ventricle while an arterial blood sample was withdrawn. Regional blood flow was then determined using standard techniques. Risk regions and areas with microvascular obstruction were defined as those with regional blood flow <50% of remote during coronary artery occlusion and after reperfusion, respectively.

Data analysis

Images from all data sets were cross-registered using the point of insertion of the right ventricular wall in the LV anteroseptal intersection as an anatomic landmark. For each animal, only five short-axis slices from the tagged MRI dataset were used for regional functional analyses. From the original eight slices acquired, the most apical and most basal slice locations were always excluded. From the remaining six slices, based on DE images, the five consecutive short-axis locations that covered the largest volume of infarcted myocardium were selected for regional functional analyses. Each slice was divided into six segments (30 segments/animal).

Tagged images were analysed quantitatively using the user interactive program Diagnosoft HARP (Diagnosoft Inc, Palo Alto, CA).[20] For each phase, Lagrangian circumferential shortening strain was computed at the subendocardial, midwall and subepi-

Table 1 Temporal data related to tagged MR image acquisition

Dog ID	Heart rate (bpm)	Time of AVC (ms)	# phases in systole/diastole
1	86	308	14/14
2	76	352	16/16
3	92	264	12/14
4	160	198	9/6
5	142	220	10/7
6	100	264	12/12
7	130	242	11/7
8	122	242	11/9
9	97	286	13/12
10	108	242	11/11
11	92	264	12/14
12	86	286	13/15
13	103	220	10/13
14	112	264	12/9
Total	108 ± 6	261 ± 11	

AVC indicates aortic valve closure.

cardial layers of each segment. Strain rates were obtained from the strain measures by deriving strain by time information. For a given phase "*n*", the strain rate was calculated as:

$$\text{Strain rate} = (\text{Strain}_{n+1} - \text{Strain}_n)\text{temporal resolution}.$$

Peak systolic and diastolic strain rates were determined only after analysis of the strain curve and determination of the peak systolic strain. We found this stepwise approach of combining the analysis of both curves, as presented in Fig. 1, to be helpful for the correct interpretation of the strain rate curves. It is well known that the peak systolic strain rate corresponds to the steepest part of the down slope of the strain curve before the peak systolic strain. Likewise, the peak early diastolic strain rate corresponds to the steepest part of the upslope of the strain curve after the peak systolic strain (Fig. 1). Therefore, the peak systolic strain rate was determined as the most negative point in the strain rate curve preceding the peak systolic strain, and the peak diastolic strain rate as the most positive point in the early diastolic portion of the strain rate curve (during the first 200 ms after the peak systolic strain). In addition, LV rotation deformation was computed in three slices per animal (basal, mid-ventricular and apical). The basal slice rotation served as the reference for the computation of apical and mid-ventricular torsion,[16] and the values obtained were normalised for the distance between the apical or mid-ventricular slice and the basal slice. After deriving torsion data by time information, the peak untwisting rate was determined for each segment (12 segments/animal).

First-pass perfusion and delayed-enhanced data were analysed quantitatively by the user interactive program Cine-Tool (General Electric). From delayed-enhanced images, infarct extent was automatically determined by computer counting of all hyper-enhanced pixels within the myocardium, i.e., those with image intensity >2SD above mean signal intensity of a remote region in the same image. Similarly, from early perfusion images (at the time of peak myocardial contrast enhancement), microvascular obstruction areas were automatically determined as the sum of all hypo-enhanced pixels within the infarcted myocardium, i.e., those with image intensity <2SD below mean signal intensity of remote myocardium.

For each animal, the 30 myocardial segments were divided into four categories according to the degree of ischaemic injury sustained during coronary occlusion and reperfusion. Transmural infarction segments were defined as those with delayed-enhancement involving $\geqslant$ 50% of their areas, subendocardial infarction segments as those with involvement of <50% of their areas by delayed-enhancement, and risk region segments as those without any involvement by delayed-enhancement, but with regional blood flow measured by radioactive microspheres <50% of remote during coronary artery occlusion. All other

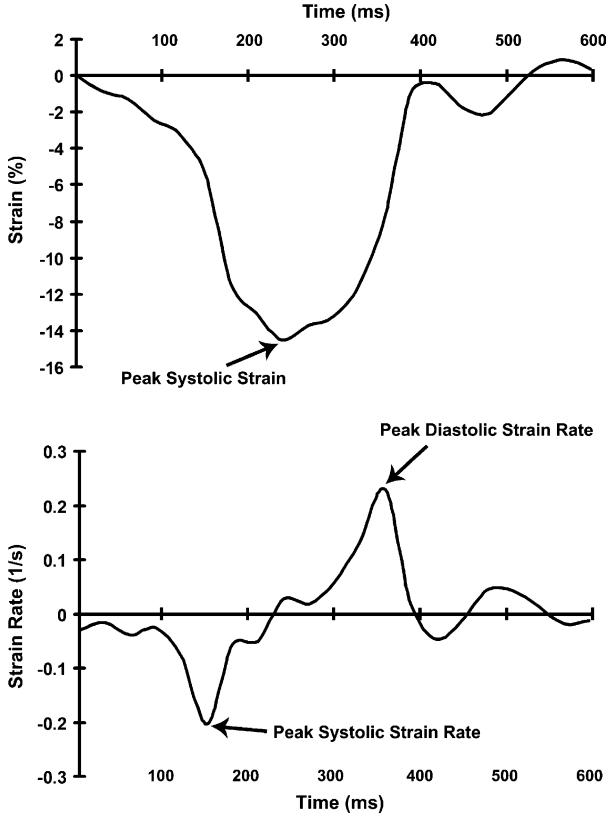

Fig. 1 Representative strain (upper) and strain rate (lower) profiles from a remote segment. This example demonstrates a typical strain pattern with normal peak systolic strain, and the corresponding strain rate curve, with normal peak systolic and diastolic strain rates.

regions were considered remote segments. Moreover, all myocardial infarction segments were further subdivided into those with and without microvascular obstruction.

Statistical analysis

All continuous values are reported as means ± SEM. Simple linear regression analysis was used to compare continuous variables in segments with different degrees of ischaemic injury after AMI. The observations were regarded as independent *across* dogs, but not *within* dogs (STATA 7.0, College Station, TX). The Huber/White/sandwich estimator of variance was used in order to take into account the correlation within dogs.[21] The reproducibility of strain and strain rate measurements were assessed using the method described by Bland and Altman.[22] All tests were two-tailed and a value of $P<0.05$ was considered indicative of statistical significance.

Results

Myocardial infarction was identified by delayed-enhancement MRI in all 14 dogs 24 h after reperfusion and involved a total of 177 segments (95 transmural and 82 subendocardial infarction segments). Based on regional myocardial blood flow measured by radioactive microspheres, a total of 80 segments were considered to be risk region segments. The remaining 163 segments were considered as remote. Microvascular obstruction, defined as hypo-enhanced regions on first-pass perfusion images, was present in 13 of the 14 dogs and involved a total of 86 myocardial infarction segments (72 transmural and 14 subendocardial infarction segments). There was a high degree of agreement between microvascular obstruction extent measured by first-pass perfusion MRI and by radioactive microspheres ($r=0.90$, $P<0.001$).

The results reported in the text are derived from midwall analysis. The results from subendocardial and subepicardial analyses are presented in Fig. 2. In addition, the time from R wave to peak systolic strain and peak systolic and diastolic strain rates is presented in Table 2.

Regional systolic function

Peak systolic circumferential strain and strain rate were measured in 391 (93%) of all 420 segments. Segments with AMI showed decreased regional systolic contractility when compared to remote areas 24 h after reperfusion (Figs. 2 and 3). Peak systolic strain was significantly decreased in both transmural and subendocardial infarction segments when compared to remote ($-2.5\pm0.5\%$ and $-6.0\pm0.9\%$ versus $-13.1\pm0.8\%$, $P<0.001$). Similarly, peak systolic strain rate was decreased in these segments compared to remote areas (-0.11 ± 0.12 s^{-1} and -0.82 ± 0.16 versus -2.15 ± 0.12 s^{-1}, $P<0.001$). Moreover, transmural AMI segments displayed greater reduction of peak systolic strain and strain rate than segments with subendocardial infarction ($P<0.01$) (Fig. 2). Risk region segments, on the other hand, demonstrated preserved regional systolic function 24 h after reperfusion, i.e., both peak systolic strain ($-12.1\pm0.7\%$) and strain rate (-2.05 ± 0.14 s^{-1}) were not significantly different from remote measures.

Regional diastolic function

Since the level of noise increases in late cardiac cycle phases due to the phenomenon of tag fading, peak diastolic strain rate could be measured in 339 (81%) of all 420 segments. Segments with AMI, in addition to regional systolic dysfunction, showed significant diastolic impairment, expressed as decreased myocardial relaxation in early diastole (Figs. 2 and 3). Indeed, peak diastolic strain rate was reduced in segments with either transmural or subendocardial infarction when compared to remote (1.26 ± 0.07 s^{-1} and 1.50 ± 0.09 versus 2.99 ± 0.13 s^{-1}, $P<0.001$). Despite their preserved regional systolic contractility, risk region segments also displayed significant regional diastolic dysfunction 24 h after reperfusion (peak diastolic strain rate $=1.62\pm0.14$ s^{-1}, $P<0.001$ versus remote) (Fig. 2).

The results obtained from the analysis of LV untwisting in early diastole are presented in Fig. 4. Importantly, these results demonstrate the same pattern of regional diastolic dysfunction in infarcted segments and non-infarcted risk regions described for strain rate analysis (Figs. 2 and 4).

Microvascular obstruction and regional function

To evaluate the effect of microvascular obstruction ("no-reflow") on regional systolic and diastolic function, all segments with AMI were divided into those with early hypo-enhancement on first-pass perfusion images and those with preserved microvascular perfusion. After controlling for segmental infarct extension, segments with areas of microvascular obstruction displayed reduced peak systolic strain ($-2.5\pm0.6\%$ versus $-5.7\pm0.7\%$, $P<0.05$), peak systolic strain rate (-0.07 ± 0.14 versus -0.79 ± 0.15 s^{-1}, $P<0.05$) and peak diastolic strain rate (1.19 ± 0.08 versus 1.54 ± 0.10 s^{-1}, $P<0.05$) when compared to AMI segments not affected by no-reflow.

Reproducibility

Fourteen segments, one for each animal, were randomly selected and both strain and strain rate analyses were repeated by another investigator and by the same investigator at a later time. The mean interobserver and intraobserver differences (bias) and repeatability coefficients (±2SD) are summarised in Table 3.

Discussion

To our knowledge, this is the first study to directly assess regional systolic and, particularly, regional

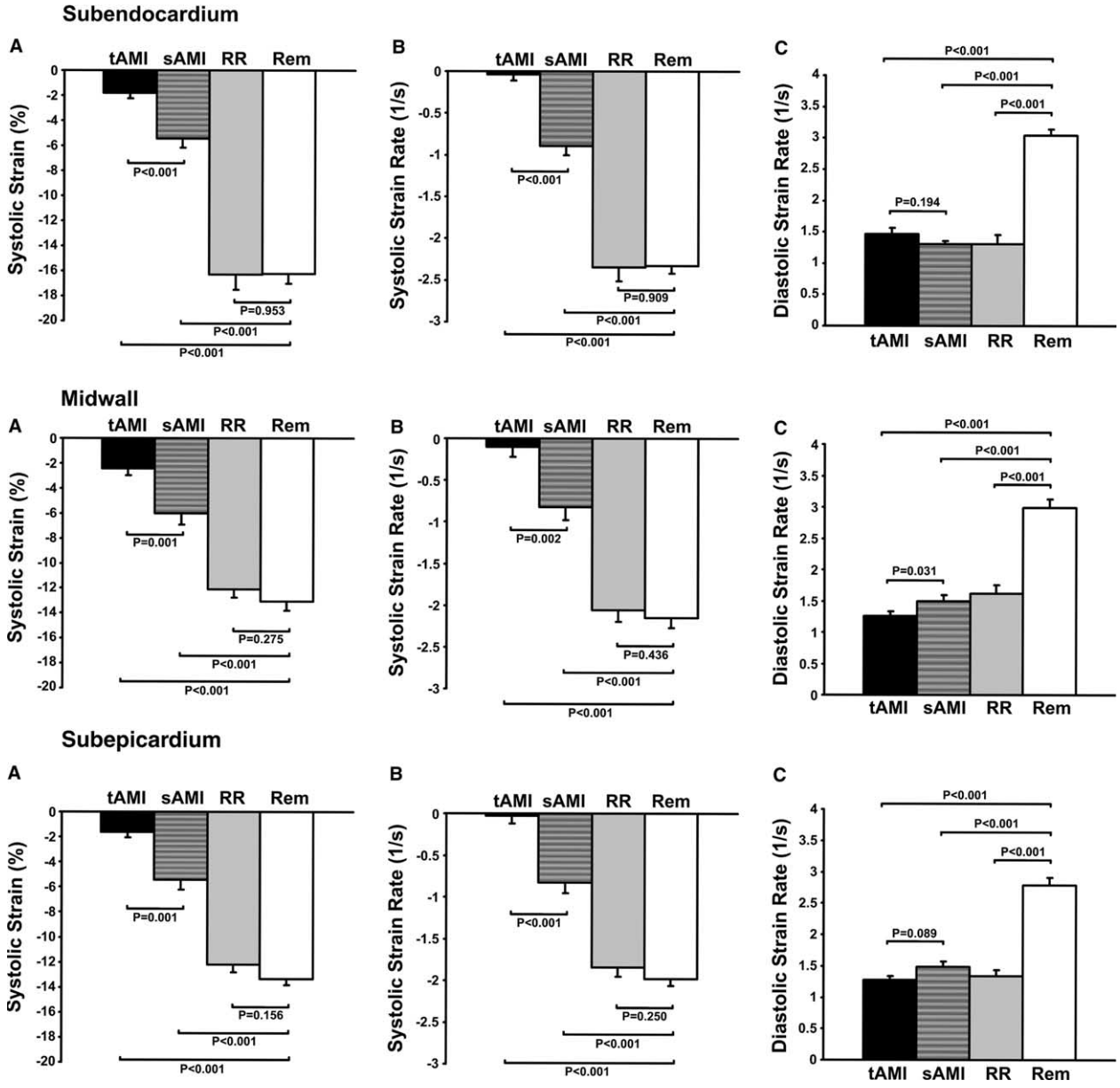

Fig. 2 Bar graphs illustrating magnitude (mean ± SEM) of peak circumferential systolic strain (A), systolic strain rate (B) and diastolic strain rate (C) in regions with different degrees of myocardial injury after reperfused AMI. The data from three myocardial layers are presented: subendocardium (top), midwall (middle) and subepicardium (bottom). Rem indicates remote area; RR, risk region; sAMI, subendocardial AMI; tAMI, transmural AMI.

diastolic function in areas with different degrees of myocardial injury after AMI using strain rates measured by tagged MRI. Our results can be summarised as follows:

1. Segments with AMI, either transmural or subendocardial, have impaired systolic and diastolic regional function, expressed as reduced peak systolic strain and peak systolic and diastolic strain rates.
2. Non-infarcted injured segments with preserved regional systolic contractility have persistent regional diastolic dysfunction 24 h after reperfusion.
3. Among AMI segments, the presence of microvascular obstruction is related to further impairment of both systolic and diastolic regional function.

Regional systolic function

The assessment of regional systolic function after AMI by strain quantification has been extensively studied, both in animals[14,23,24] and in patients.[20,25] In all studies, systolic strain in segments with myocardial infarction was reduced compared to remote, which is in accordance to our findings. In addition, our study demonstrates that segments with transmural infarction have greater depression of systolic strain and strain rate than segments with subendocardial infarction (Fig. 2). We also observed that the presence of microvascular obstruction, a marker of severe ischaemic injury, is related to further impairment of regional systolic contractility, which is in agreement with previous studies.[23]

Table 2 Time from R wave to peak systolic strain and peak systolic and diastolic strain rates

	Transmural infarction	Subendocardial infarction	Risk region	Remote area
Time to peak systolic strain (ms)	256 ± 9*	240 ± 10	248 ± 9	232 ± 14
Time to peak systolic strain rate (ms)	186 ± 8**	170 ± 14****	154 ± 5	150 ± 8
Time to peak diastolic strain rate (ms)	362 ± 10***	345 ± 18	340 ± 9	330 ± 14

* $P < 0.05$.
** $P < 0.001$.
*** $P < 0.01$.
**** $P = 0.058$ versus remote.

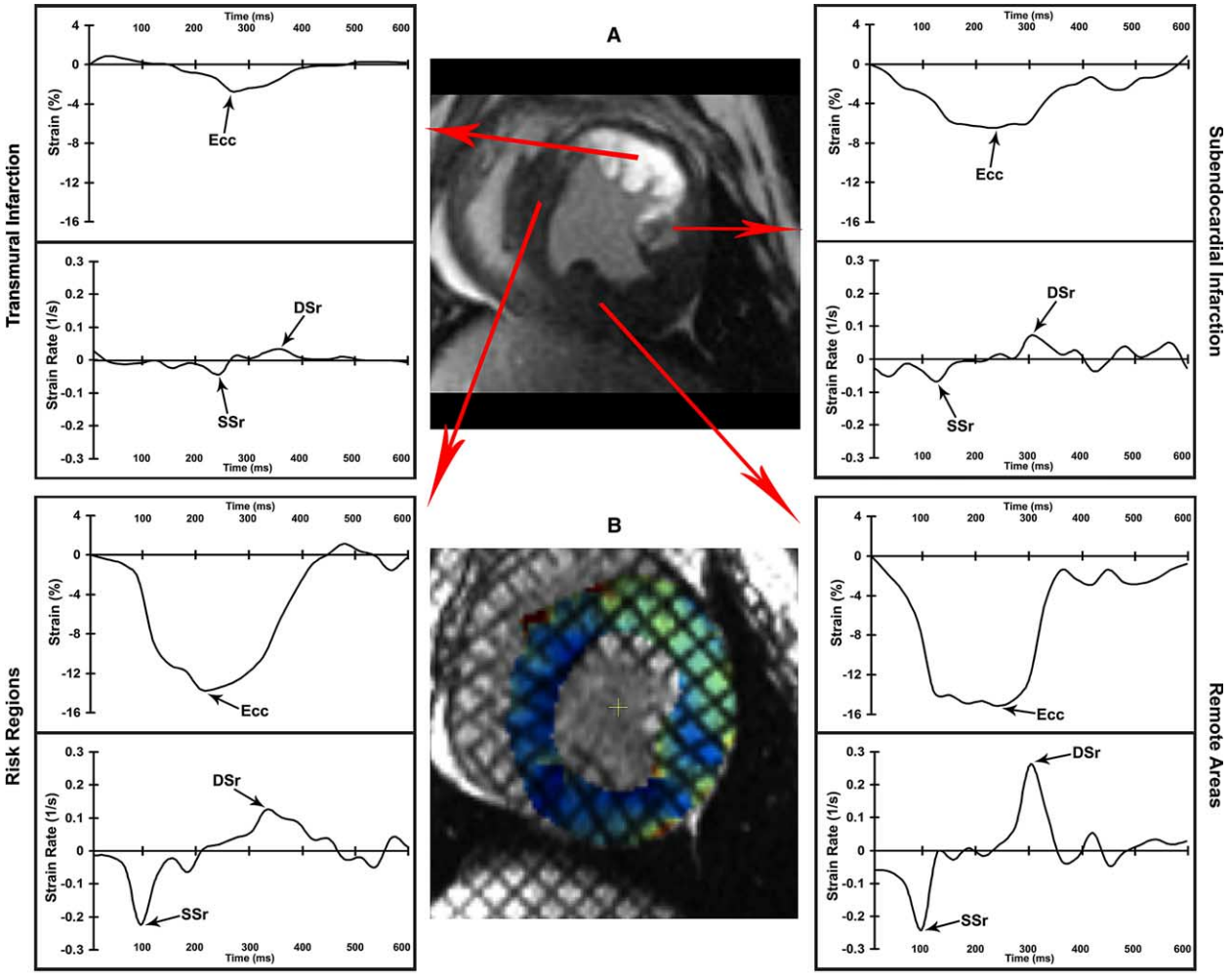

Fig. 3 Representative circumferential strain and strain rate profiles from 4 different segments: transmural infarction (upper left), subendocardial infarction (upper right), risk region (lower left) and remote area (lower right). Note that myocardial infarction segments have reduced peak systolic strain (Ecc) and systolic (SSr) and diastolic (DSr) strain rates compared to remote area. Risk region segments also display regional diastolic dysfunction (reduced DSr), but have preserved regional systolic contractility (normal Ecc and SSr). (A) Illustrative mid-ventricular short-axis delayed-enhanced image showing a large anterior myocardial infarction. (B) Corresponding strain encoded image at a late systolic phase showing the normally contracting myocardium in blue and the dysfunctional myocardium in green.

In our model, risk region segments represented non-infarcted myocardial areas that were subjected to reversible ischaemic damage. Therefore, our finding that these segments exhibited preserved systolic contractility 24 h after reperfusion should be analysed under the light of the myocardial stunning concept. The phenomenon of myocardial stunning after an ischaemic insult is defined as the mechanical dysfunction that persists after reperfusion despite the absence of irreversible damage and despite return of normal or near-normal perfusion.[3,4] The capability of delayed-enhanced MRI to accurately distinguish areas of reversible ischaemic damage from necrotic tissue, combined with the ability of tagged MRI to quantify regional function, makes cardiac MRI examination well-suited for the detailed characterisation of this pathophysiological process. It is important to highlight that, in our model, AMI segments were partially composed of irreversibly injured necrotic tissue, but

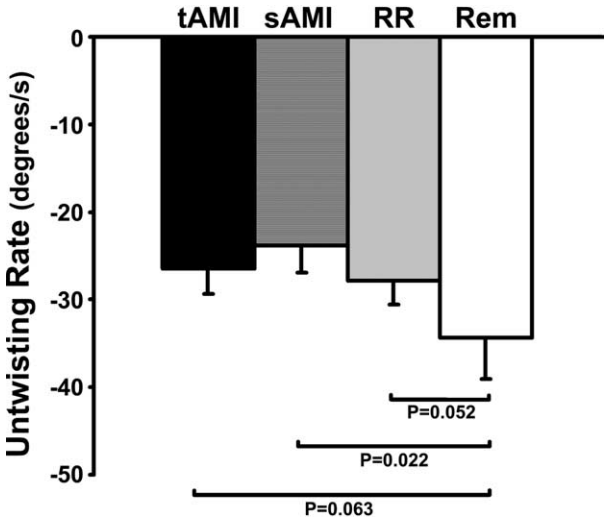

Fig. 4 Bar graph illustrating magnitude of peak untwisting rate in regions with different degrees of myocardial injury after reperfused AMI. Rem indicates remote area; RR, risk region; sAMI, subendocardial AMI; tAMI, transmural AMI.

were also partially composed of non-infarcted but ischaemically injured myocardium (particularly subendocardial infarction segments). The degree of ischaemic injury imposed on the non-infarcted myocardial tissue within these segments was severe enough to result in systolic mechanical dysfunction up to 24 h after reperfusion. The adjacent risk region segments also suffered from ischaemic injury, but not of enough magnitude to cause persistent systolic stunning up to 24 h after the ischaemic insult. Therefore, we believe that our study fits the experimental model of stunning after a partly reversible (no necrosis) plus partly irreversible (some areas of necrosis) episode of regional ischaemia in vivo as described by Kloner et al.[3]

In a previous study, Croisille et al.,[24] reported reduced peak systolic strains in non-infarcted risk region segments when compared to remote regions 48 h after reperfusion. However, that finding was based on radial and maximal principal E1 (greater thickening) strains, and not on circumferential strain as is the case of the present study. When circumferential strain was examined, no difference in regional systolic function was detected between risk region segments and remote areas, which is in accordance with our findings.

The time-to-peak systolic strain and strain rate were significantly higher in segments with transmural AMI than in remote areas. A trend towards higher time-to-peak systolic strain rate was also observed among segments with subendocardial infarction (Table 2). We believe these findings might be related to the phenomenon of post-systolic shortening.[26] Indeed, as many as 73% (61/84) of transmural and 56% (42/75) of subendocardial infarction segments only reached peak systolic strain after aortic valve closure. In contrast, only 23% (18/77) of risk region and 22% (34/155) of remote segments displayed peak systolic strain in early diastole. As demonstrated by Skulstad et al.,[26] post-systolic shortening can result from two distinct mechanisms: passive recoil or active contraction. Although we believe our finding of post-systolic shortening in segments with transmural infarction is probably related to the first mechanism and reflects only passive recoil, we suspect the finding of post-systolic shortening in subendocardial infarction segments could be the result of active myocardial contraction.

Regional diastolic function

In the present study, using strain rate measured by tagged MRI, we were able to demonstrate that regions that suffered significant ischaemic injury during coronary occlusion and reperfusion displayed persistent regional diastolic impairment. Indeed, AMI segments showed both systolic and diastolic regional dysfunction and these findings are in accordance with previous reports.[9,13] By contrast, risk region segments only exhibited diastolic impairment, but not systolic dysfunction 24 h after reperfusion. A previous study by Przyklenk et al.,[5] described the concept that the myocardial stunning phenomenon is not limited to regional systolic impairment, but, in fact, also has a diastolic component. Moreover, as suggested in a previous study by Wijns et al.,[27] the diastolic component would have a lower ischaemic injury threshold for its occurrence than the systolic component, i.e., regions that suffered lesser degrees of ischaemic injury during coronary artery occlusion, may develop prolonged isolated diastolic dysfunction despite restoration of coronary blood flow and recovery of regional systolic contractility. In that study, brief episodes of coronary artery occlusion (<1 min) were applied and patients were followed for a short period of time after coronary angioplasty. Persistence of diastolic dysfunction was documented for up to 12 min after the ischaemic insult. In our experimental model, a 90-min coronary artery occlusion followed by reperfusion was performed and we were able to evaluate regional contractility and relaxation in a wide range of ischaemic injury levels. Moreover, we demonstrate the persistence of regional diastolic impairment in non-infarcted injured segments for as long as 24 h after the ischaemic episode. However, since we did not follow regional diastolic functional recovery beyond 24 h of reperfusion, we were not able to conclusively define whether this finding constitutes persistence of diastolic stunning (with eventual diastolic functional recovery), or whether this actually constitutes irreversible diastolic functional compromise.

Table 3 Reproducibility for strain and strain rate measurements

	Systolic strain (%)	Systolic strain rate (s^{-1})	Diastolic strain rate (s^{-1})
Interobserver variability	0.7±6.8	0.16±1.39	0.12±1.15
Intraobserver variability	−0.4±5.9	0.06±0.97	−0.16±0.99

Data are presented as mean differences±2SD (bias±repeatability coefficient).

In view of the aforementioned concept that ischaemic injury causes regional diastolic dysfunction, it is intuitive to hypothesise that microvascular obstruction areas are characterised by even greater diastolic functional impairment. In fact, it has been shown that both diastolic dysfunction[28] and microvascular obstruction[29] are related to increased post-infarct LV remodelling. However, to our knowledge, this is the first study demonstrating a direct relationship between microvascular obstruction and greater post-infarct LV diastolic dysfunction.

Limitations

Due to the phenomenon of tag fading in later phases of the cardiac cycle, the positive strain rate related to atrial contraction ("a" wave strain rate) was not evaluated in this study. In addition, tagging protocols with two breath-holds per slice location, that could potentially generate tags that persist with good signal-to-noise ratio throughout the whole cardiac cycle, such as the C-SPAMM pulse sequence, were not used in the present study.

In order to correlate regional LV functional data with the different contrast-enhancement patterns, each slice was divided into six equal segments. However, some segments might not be uniformly composed of just 1 type of myocardial injury, but, in fact, might constitute a mixture of different types. This could potentially lead to averaging of the data. In fact, since myocardial damage does not respect arbitrary segmentation models, this limitation will also be present in the great majority of studies that related regional LV function and different indexes of regional myocardial damage. Importantly, since we were able to clearly identify the differences between segments from each myocardial injury category, we do not believe this limitation had a significant influence on our overall results.

It is also important to highlight that we only assessed the effect of ischaemic injury on regional LV function up to 24 h after coronary occlusion and reperfusion. Therefore, we did not investigate how regional diastolic function relates to long-term outcomes, such as post-infarct LV remodelling or regional myocardial viability. Further studies are required to address these important questions.

Conclusions

This study demonstrates that reversibly injured regions can present with persistent regional diastolic dysfunction despite complete recovery of regional systolic contractility after reperfused AMI. It also demonstrates that segments with AMI involvement, either transmural or subendocardial, display significant impairment of both systolic and diastolic regional function. Importantly, this is the first study showing that, in addition to regional systolic dysfunction, the presence of microvascular obstruction is also related to regional diastolic impairment. Finally, this study demonstrates that regional diastolic function can be quantified in detail using strain rate analysis by tagged MRI.

Acknowledgement

This work was supported by NIH/NHLBI Grants RO1-HL63439 and RO1-HL66075-01 and by Datascope Corporation, Mahwah, NJ.

References

1. Lima JA, Judd RM, Bazille A et al. Regional heterogeneity of human myocardial infarcts demonstrated by contrast-enhanced MRI. Potential mechanisms. *Circulation* 1995;**92**:1117–25.
2. Stugaard M, Brodahl U, Torp H et al. Abnormalities of left ventricular filling in patients with coronary artery disease: assessment by colour M-mode Doppler technique. *Eur Heart J* 1994;**15**:318–27.
3. Kloner RA, Bolli R, Marban E et al. Medical and cellular implications of stunning, hibernation, and preconditioning: an NHLBI workshop. *Circulation* 1998;**97**:1848–67.
4. Heyndrickx GR, Wijns W, Melin JA. Regional wall motion abnormalities in stunned and hibernating myocardium. *Eur Heart J* 1993;**14**(Suppl A):8–13.
5. Przyklenk K, Patel B, Kloner RA. Diastolic abnormalities of postischemic stunned myocardium. *Am J Cardiol* 1987;**60**:1211–3.
6. Diamond G, Forrester JS. Effect of coronary artery disease and acute myocardial infarction on left ventricular compliance in man. *Circulation* 1972;**45**:11–9.
7. Poulsen SH, Jensen SE, Gotzsche O et al. Evaluation and prognostic significance of left ventricular diastolic function assessed by Doppler echocardiography in the early phase of a first acute myocardial infarction. *Eur Heart J* 1997;**18**:1882–9.
8. Nijland F, Kamp O, Karreman AJ et al. Prognostic implications of restrictive left ventricular filling in acute myocardial infarction: a serial Doppler echocardiographic study. *J Am Coll Cardiol* 1997;**30**:1618–24.
9. Tyberg JV, Forrester JS, Wyatt HL et al. An analysis of segmental ischemic dysfunction utilizing the pressure-length loop. *Circulation* 1974;**49**:748–54.
10. Bonow RO, Vitale DF, Bacharach SL et al. Asynchronous left ventricular regional function and impaired global diastolic filling in patients with coronary artery disease: reversal after coronary angioplasty. *Circulation* 1985;**71**:297–307.
11. Garcia MJ, Thomas JD, Klein AL. New Doppler echocardiographic applications for the study of diastolic function. *J Am Coll Cardiol* 1998;**32**:865–75.
12. Garcia-Fernandez MA, Azevedo J, Moreno M et al. Regional diastolic function in ischaemic heart disease using pulsed wave Doppler tissue imaging. *Eur Heart J* 1999;**20**:496–505.
13. Garot J, Derumeaux GA, Monin JL et al. Quantitative systolic and diastolic transmyocardial velocity gradients assessed by M-mode colour Doppler tissue imaging as reliable indicators of regional left ventricular function after acute myocardial infarction. *Eur Heart J* 1999;**20**:593–603.
14. Lima JA, Jeremy R, Guier W et al. Accurate systolic wall thickening by nuclear magnetic resonance imaging with tissue tagging: correlation with sonomicrometers in normal and ischemic myocardium. *J Am Coll Cardiol* 1993;**21**:1741–51.
15. Clark NR, Reichek N, Bergey P et al. Circumferential myocardial shortening in the normal human left ventricle. Assessment by magnetic resonance imaging using spatial modulation of magnetization. *Circulation* 1991;**84**:67–74.
16. Rademakers FE, Buchalter MB, Rogers WJ et al. Dissociation between left ventricular untwisting and filling. Accentuation by catecholamines. *Circulation* 1992;**85**:1572–81.
17. Edvardsen T, Gerber BL, Garot J et al. Quantitative assessment of intrinsic regional myocardial deformation by Doppler strain rate echocardiography in humans: validation against three-dimen-

sional tagged magnetic resonance imaging. *Circulation* 2002;**106**: 50–6.
18. Slavin GS, Wolff SD, Gupta SN et al. First-pass myocardial perfusion MR imaging with interleaved notched saturation: feasibility study. *Radiology* 2001;**219**:258–63.
19. Simonetti OP, Kim RJ, Fieno DS et al. An improved MR imaging technique for the visualization of myocardial infarction. *Radiology* 2001;**218**:215–23.
20. Garot J, Bluemke DA, Osman NF et al. Fast determination of regional myocardial strain fields from tagged cardiac images using harmonic phase MRI. *Circulation* 2000;**101**:981–8.
21. White HA. Heteroskedasticity-consistent covariance-matrix estimator and a direct test for heteroskedasticity. *Econometrica* 1980;**48**:817–38.
22. Bland JM, Altman DG. Statistical methods for assessing agreement between two methods of clinical measurement. *Lancet* 1986;**1**:307–10.
23. Gerber BL, Rochitte CE, Bluemke DA et al. Relation between Gd-DTPA contrast enhancement and regional inotropic response in the periphery and center of myocardial infarction. *Circulation* 2001;**104**:998–1004.
24. Croisille P, Moore CC, Judd RM et al. Differentiation of viable and nonviable myocardium by the use of three-dimensional tagged MRI in 2-day-old reperfused canine infarcts. *Circulation* 1999;**99**: 284–91.
25. Gotte MJ, van Rossum AC, Twisk JWR et al. Quantification of regional contractile function after infarction: strain analysis superior to wall thickening analysis in discriminating infarct from remote myocardium. *J Am Coll Cardiol* 2001;**37**: 808–17.
26. Skulstad H, Edvardsen T, Urheim S et al. Postsystolic shortening in ischemic myocardium: active contraction or passive recoil. *Circulation* 2002;**106**:718–24.
27. Wijns W, Serruys PW, Slager CJ et al. Effect of coronary occlusion during percutaneous transluminal angioplasty in humans on left ventricular chamber stiffness and regional diastolic pressure-radius relations. *J Am Coll Cardiol* 1986;**7**: 455–63.
28. Cerisano G, Bolognese L, Carrabba N et al. Doppler-derived mitral deceleration time: an early strong predictor of left ventricular remodeling after reperfused anterior acute myocardial infarction. *Circulation* 1999;**99**:230–6.
29. Ito H, Maruyama A, Iwakura K et al. Clinical implications of the 'no reflow' phenomenon. A predictor of complications and left ventricular remodeling in reperfused anterior wall myocardial infarction. *Circulation* 1996;**93**:223–8.